THE EFFECT OF σ-PHASE PRECIPITATION AT 800°C ON THE CORROSION RESISTANCE IN SEA-WATER OF A HIGH ALLOYED DUPLEX STAINLESS STEEL

M. E. WILMS,* V. J. GADGIL,† J. M. KROUGMAN* and F. P. IJSSELING*

*Marine Materials Engineering Laboratory of the Royal Netherlands Naval College, P. O. Box 10000, 1780 CA Den Helder, The Netherlands
†Centre for Materials Research (CMO), University of Twente, EL-TN Gebouw, P. O. Box 217, 7500 AE, The Netherlands

Abstract—Super-duplex stainless steels are recently developed high alloyed stainless steels that combine good mechanical properties with excellent corrosion resistance. Because of a high content of chromium and molybdenum, these alloys are susceptible to σ-phase precipitation during short exposure to temperatures between 650 and 950°C. The effect of 800°C aging on σ-phase formation and on the mechanical properties of a super-duplex stainless steel have been reported previously by the authors.[1] This investigation concerns the effect of σ-phase precipitation at 800°C on the corrosion behaviour in sea-water and comprises anodic polarization scans and potentiostatic crevice corrosion tests. A serious deterioration of the corrosion resistance is found after aging times longer than 7 min, resulting in a drop of both the critical crevice corrosion temperature (CCT) and the breakdown potential (E_{bd}). The initiation of localized corrosion takes place next to the σ-phase, in the newly formed secondary austenite (γ_2).

INTRODUCTION

DUPLEX stainless steels have a microstructure which consists of about equal amounts of ferrite and austenite. These materials are attractive for numerous applications because of high strength,[2,3] good corrosion resistance[4] and ease in fabrication.[2] Applications in more corrosive environments have created a demand for alloys with better corrosion resistance. This led to the development of higher alloyed duplex stainless steels, referred to as super-duplex stainless steels.[5,6] The super-duplex stainless steels contain higher Cr (*ca* 25%), Ni (*ca* 7%), Mo (*ca* 4%) and N (*ca* 0.3%). These alloying additions provide better mechanical properties and improved resistance to localized corrosion and stress corrosion cracking (SCC) as compared to the normal duplex stainless steels.[7–9]

The increase in the content of the elements Cr, Ni and Mo accelerates the precipitation of σ-phase during exposure to high temperatures (700–1000°C). This σ-phase formation leads to serious embrittlement.[10] At 800°C other precipitates (nitrides, chi-phase) are also formed in super-duplex stainless steel. The precipitation of σ-phase is found to be the most rapid and it has the strongest influence on corrosion resistance.[11]

The aim of the reported investigation is to study the effect of σ-phase precipitation at 800°C on the resistance to localized corrosion in sea-water of a super-duplex stainless steel.

TABLE 1.   CHEMICAL COMPOSITION OF THE SUPER-DUPLEX STAINLESS STEEL
INVESTIGATED

Cr	Ni	Mo	N	C	Si	Mn	P	S
24.01	7.11	3.89	0.29	0.018	0.22	0.31	0.018	0.001

EXPERIMENTAL METHOD

The chemical composition of the alloy investigated, is given in Table 1. The material was in the form of 3 mm cold rolled plate, solutionized at 1075°C for 10 min, followed by water quenching.

Heat treatment

Specimens of 20 × 20 mm were cut from the plate and aged at 800°C. The aging time was varied between 2 and 1500 min. The temperature was controlled with a chromel–alumel thermocouple, welded to the surface by percussion welding. For short aging times a radiation heated tube furnace was used, with a nitrogen atmosphere. For aging times of 30 min and longer, an electric muffle furnace was used and the specimens were wrapped in stainless steel foils for protection from oxidation. After aging, all the specimens were water quenched.

The microstructure of the specimens was investigated by optical microscopy. Lichtnegger and Bloch (20 g NaF, 0.5 g $K_2S_2O_5$, 100 ml H_2O at 50°C) and Groesbeck's reagent (4 g $KMnO_4$, 4 g NaOH, 100 ml H_2O at 70°C) were used for metallography. A scanning electron microscope with a Robinson back-scattered electron detector was used to characterize the initiation sites of corrosion attack. Details regarding metallography and the estimation of the volume fraction of σ-phase are found in Ref. 1.

Corrosion tests

To investigate the influence of the σ-phase precipitation on the corrosion behaviour, the following experimental techniques were used: (a) anodic polarization scans and (b) potentiostatic exposure.
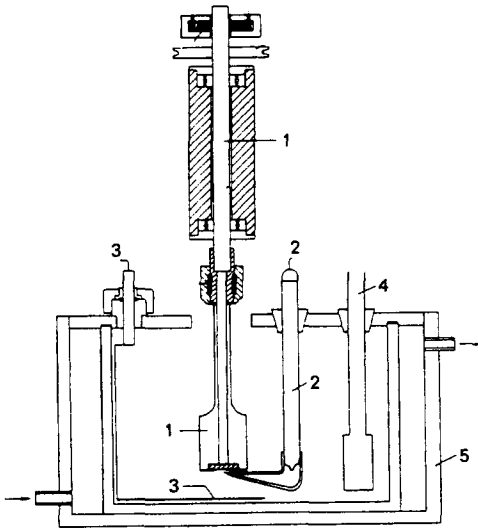
1. rotating electrode
2. reference electrode
3. auxiliary electrode
4. tube for nitrogen bubbling
5. double walled cell for temperature control

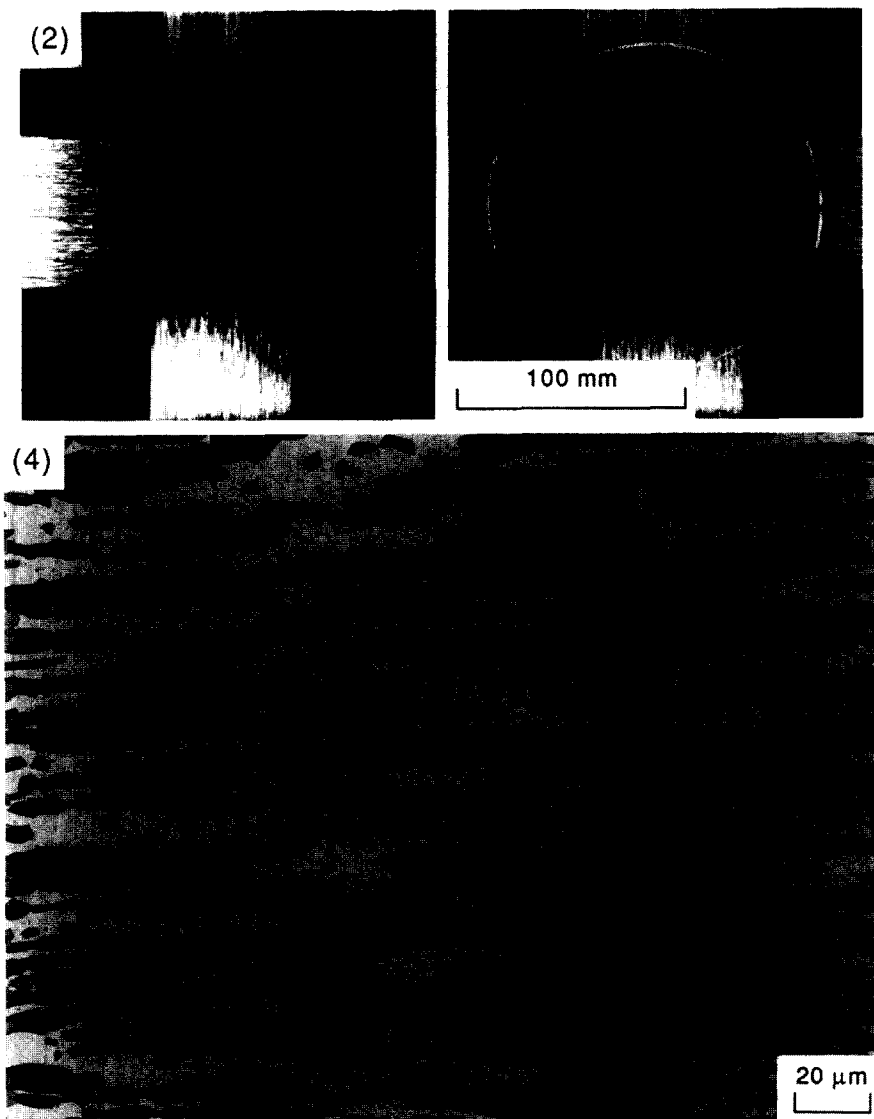FIG. 1.   Experimental arrangement used for polarization scans.

FIG. 2. Scratched sample as used in the potentiostatic expositions.

FIG. 4. Microstructure of the as-received material. γ appears as a dark phase, α is light. (Lichtnegger and Bloch reagent; magnification 500 ×).
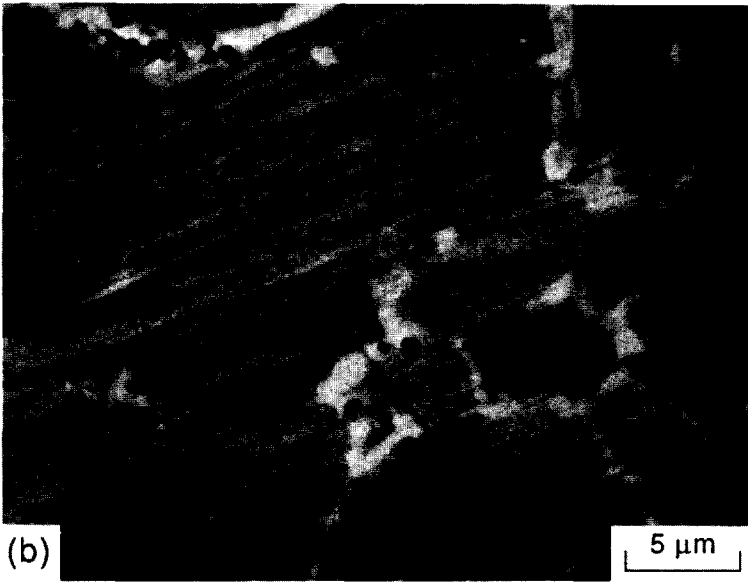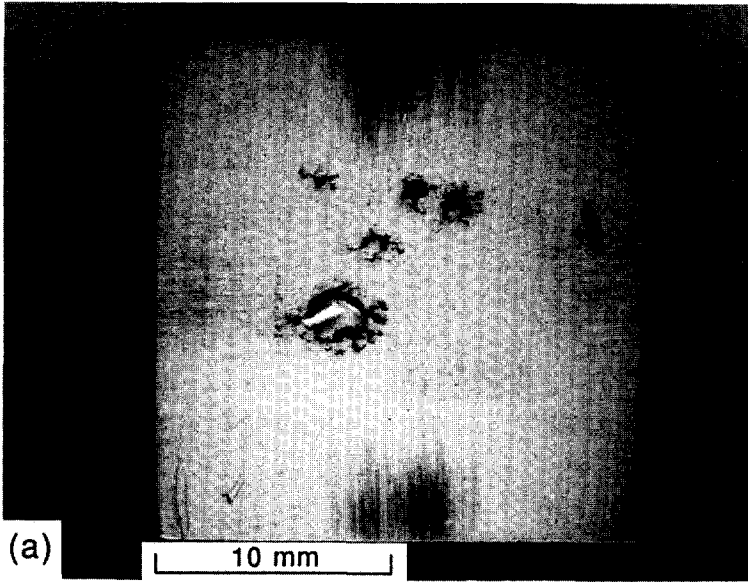
(a)

| 10 mm |

(b)

5 μm

FIG. 8.   Scanning electron microscope picture of the corrosion attack after potentiostatic exposition of material aged for 10 min (a + b) and 1500 min (c + d).
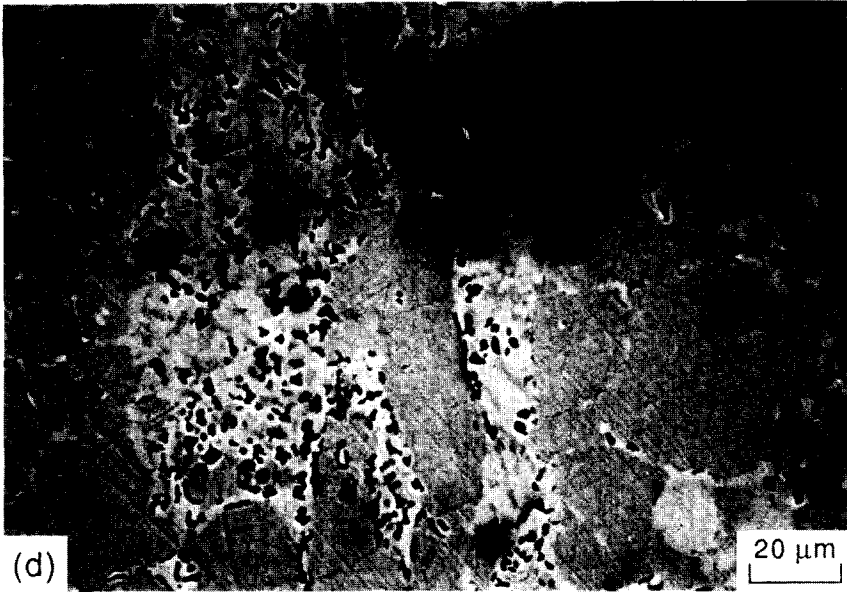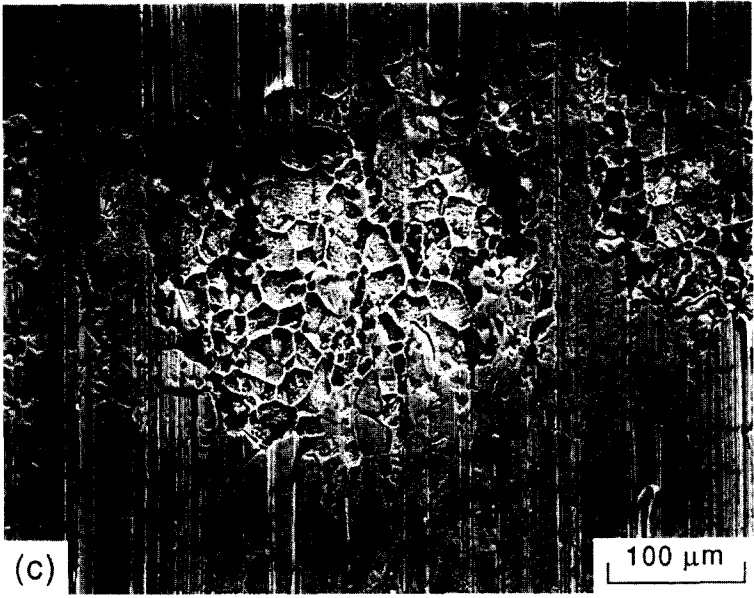
874

(c)

100 μm

(d)

20 μm

Fig. 8. *Continued.*

875

1. graphite electrode
2. heating element
3. contact thermometer
4. auxiliary electrode
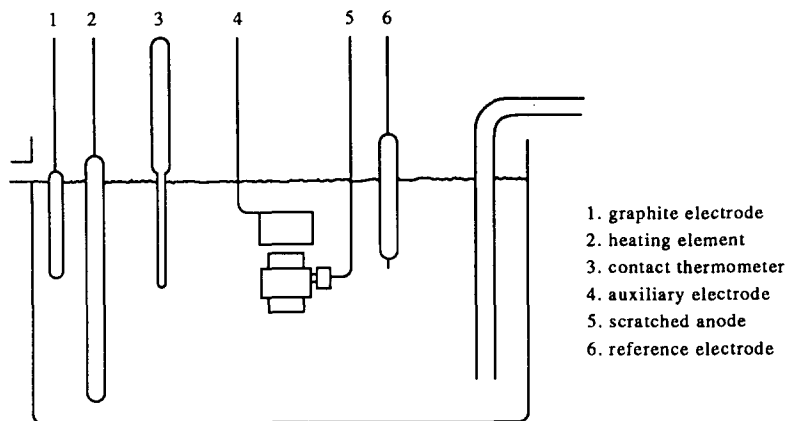5. scratched anode
6. reference electrode

FIG. 3.   Experimental arrangement used for potentiostatic expositions.

Polarization scans

Anodic polarization scans were carried out with a rotating electrode in a simulated crevice environment. The experimental arrangement can be seen in Fig. 1. The surface of the specimens was prepared by grinding with 220 grit SiC paper. A surface of 1 cm^2 was exposed to the environment during the test. The specimens were mounted in rotating holders. The specimens were rotated at a speed of 1500 rpm. An EG&G PARC model 173 potentiostat provided with a type 276 interface for computer control was used to record the polarization curve at a scan speed of 20 mV min^{-1}. A saturated calomel electrode (SCE) and a platinum disk electrode were used as reference and counter electrode, respectively. Dry nitrogen was bubbled through the solution during the test to exclude oxygen from the simulated crevice environment. The environment used during the test was artificial sea-water (as per ASTM standard D-1141-52) with addition of 263 g l^{-1} NaCl and the pH adjusted to pH 1 by HCl. Tests were carried out at a temperature of 40°C. The scans were started at −600 mV(SCE) and stopped when the anodic current density reached a value of 50 μA cm^{-2}. Further details of the test method are reported elsewhere.[12]

From the polarization curves the E_{bd} (breakdown potential) and the i_c (critical current density) were
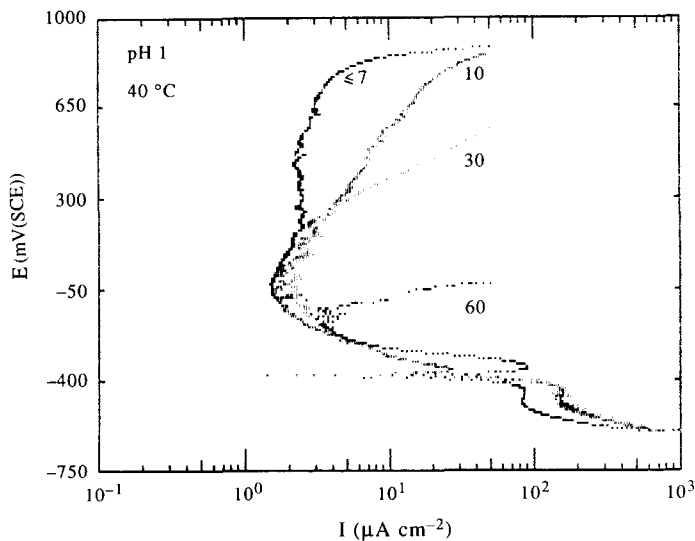

FIG. 5.   Polarization scans in simulated crevice environment of as-received material and material aged for 7–60 min.
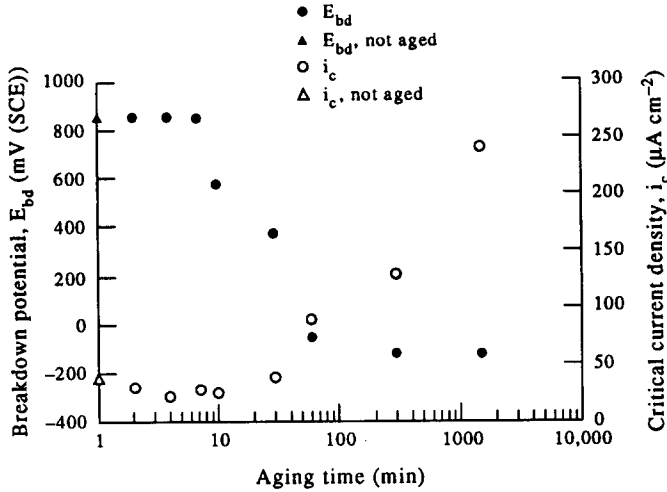
FIG. 6.   Breakdown potential (E_{bd}) and critical current density (i_c) as function of the aging
time.

determined. The E_{bd} is defined here as the potential value at which a current density of $10 \mu A$ cm^{-2} is
reached. The value of i_c is the largest anodic current density that is measured while increasing the
potential, before the passive area is reached.

Potentiostatic exposure

This test aims to determine the critical crevice corrosion temperature (CCT). CCT is defined as the
highest temperature at which the material tested remains free from crevice corrosion. The test
environment was brackish sea-water pumped up from a depth of 6 m from the harbour of Den Helder
(pH 7.8–8.1). During the test runs, which lasted 3 h, the potential was kept constant at a value of
500 mV(SCE), which is about the maximum free corrosion potential reached by stainless steel in natural
sea-water. Each test was carried out at a constant temperature. The temperature was raised in steps of
15°C for each test, starting at 10°C. The maximum testing temperature was 95°C.

Before testing, the surface of the specimens was polished with $3 \mu m$ diamond paste. Subsequently the
surface of the specimen was scratched in four directions with a 800 grit silicon carbide paper by a standard
method.[13] In this way approximately 1500 microscratches were obtained on the surface as can be seen in
Fig. 2. For testing, the specimens were mounted in special holders. In the holder the specimen was pressed
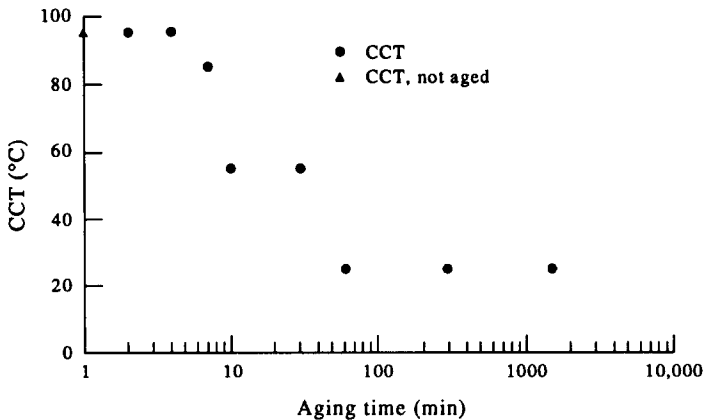

FIG. 7.   Critical crevice corrosion temperature (CCT) as function of the aging time.
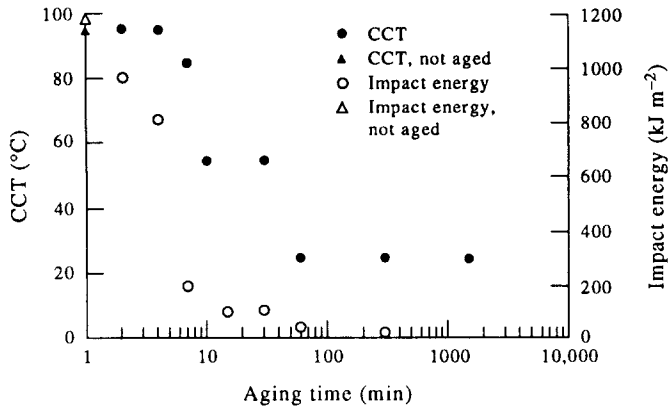
FIG. 9. Critical crevice corrosion temperature (CCT) and impact value (from Ref. 1) as function of the aging time.

against a rubber O-ring. The O-ring partially covered the microscratches. The microscratches in the macro-crevice, formed between the surface of the specimen and the O-ring, created a large number of initiation sites for crevice corrosion. The experimental arrangement can be seen in Fig. 3, while a further description of the test method can be found in Ref. 13.

The CCT was determined by taking into account the current vs time plots, total transported charge, weight loss of the specimen and maximum penetration depth.

EXPERIMENTAL RESULTS

σ-Phase transformation

The microstructure of the as-received material consists of grains of austenite (γ) and ferrite (α) matrix (Fig. 4). During aging at 800°C, σ-phase nucleates at the α/γ phase boundaries and grows into the ferrite: $\alpha \rightarrow \sigma$. After aging for 2 min, nuclei are already visible with a scanning electron microscope.

After aging for 7 min, a new phase forms from the α next to the growing σ-phase grains: secondary austenite (γ_2). The transformation proceeds as $\alpha \rightarrow \sigma + \gamma_2$. The σ-phase is rich in chromium and molybdenum. During the growth of the σ-phase, these elements diffuse from the surrounding ferrite matrix to the σ-phase. This surrounding region is depleted of these elements. The change in the composition leads to the transformation of this region to austenite phase referred to as γ_2. At longer aging times all α can be transformed to σ-phase and γ_2.

Polarization scans

The anodic polarization curves of specimens in as-received condition, and of specimens aged at 800°C for 2, 4, 7, 10, 30 and 60 min are shown in Fig. 5. The polarization curves for as-received material and for specimens aged at 2, 4 and 7 min are almost identical. The first indication of the deterioration of the corrosion resistance can be seen after aging for 10 min. The effect of aging time on the breakdown potential (E_{bd}) is shown in Fig. 6. The value of E_{bd} remains *ca* 850 mV(SCE) for aging times up to 7 min. Between 7 and 60 min of aging E_{bd} drops *ca* 1000 mV. Longer aging does not change the E_{bd} further.

The behaviour of critical current density (i_c) with respect to the aging time is shown in Fig. 6. Initially there is a slight drop of the i_c with aging time. For specimens aged above 10 min the i_c increases with increasing aging time.

Potentiostatic exposures

The results of the potentiostatic exposure tests which show CCT as function of the aging time are given in Fig. 7. The initial value of the CCT of as-received material is 95°C. As the aging time is increased, the CCT sharply drops between 4 and 60 min. Aging longer than 60 min does not lower the CCT any further.

The appearance of the localized attack after testing of specimens aged for 10 and 1500 min can be seen in Fig. 8. The type of attack is both crevice and pitting corrosion as visible in Fig. 8a. The pitting type of attack is shown in detail in Fig. 8b. This picture and the pitting attack in Fig. 8d clearly show that local corrosion is initiated adjacent to the σ-phase. The micrograph after potentiostatic exposure of specimen aged for 1500 min can be seen in Fig. 8c and d. It can be observed that the σ-phase is almost intact, while the γ-phases (in particular γ_2) are attacked.

DISCUSSION

With the formation of σ-phase a decrease of the resistance to localized corrosion is observed. This can be explained by depletion zones of Cr and Mo next to the growing σ-phase. Both these elements are found in higher concentrations in the σ-phase. During the formation of σ-phase, these elements diffuse from the surrounding zone to the growing σ-particle, thus causing localized depletion areas. These areas with lower concentrations of the elements Cr and Mo result in a lower E_{bd} and a higher i_c.

Rapid deterioration of corrosion resistance with aging time is seen after 7 min, which coincides with the formation of γ_2. This is the phase where the depletion is most severe. γ_2 is formed from depleted zones of α, next to the σ-phase. Because of faster diffusion of Cr and Mo in the α as compared to the γ, these elements are lower in the γ_2 than in the grains present in the as-received material.

The CCT and the E_{bd} both settle at a constant value after 60 min of aging, indicating that zones with a maximum depletion of Cr and Mo have formed in the γ_2 after this aging time. Only an increase in the amount of maximum depleted γ_2 is expected after further aging. This is confirmed by the i_c that rises continuously with aging times longer than 60 min. The value of i_c is connected to the average of surface conditions, while the value of the CCT and E_{bd} refer to the least resistant locations at the surface.

The adverse influence of σ-phase formation on corrosion resistance is first seen by a drop of the CCT. The E_{bd} and i_c show this effect later, as seen by comparing Figs 6 and 7. This difference may be attributed to slowness of response to critical conditions of the potentiodynamic measurement compared to the potentiostatic exposure.

Deterioration of the toughness of a super-duplex stainless steel due to σ-phase precipitation, is found to occur before reduction of corrosion resistance in sea-water. The effect of 800°C aging on the σ-phase formation and mechanical properties of a super-duplex stainless steels have been previously reported by the authors.[1] The impact value appeared to be the mechanical property deteriorating most rapidly after aging at 800°C. Even with aging for 2 min, the impact value dropped by 19%. With further aging to 7 min the drop in the impact strength was about 83% (Fig. 9). It is interesting to note that this is in contradiction with results found for corrosion resistance in a 10% $FeCl_3$ solution.[14]

Considering the corrosion resistance in sea-water, super-duplex stainless steel shows only a little reduction after aging at 800°C for 7 min. However, according to

mechanical properties (impact value), the material is completely spoilt (Fig. 9). This indicates that during σ-phase precipitation, the corrosion resistance in sea-water is not the property deteriorating first.

CONCLUSIONS

(1) The aging of high alloyed duplex stainless steel at 800°C seriously affects the resistance to localized corrosion in sea-water when aging times are longer than 7 min.

(2) The initiation of localized corrosion takes place around the σ-phase due to depletion of Cr and Mo while the σ-phase itself appears to be unaffected.

(3) The secondary austenite (γ_2), formed during the σ-phase transformation ($\alpha \rightarrow \gamma_2 + \sigma$), is the phase that is primarily attacked by localized corrosion.

(4) After aging at 800°C, duplex stainless steels show unacceptable changes in mechanical properties (embrittlement) before the corrosion resistance in sea-water is affected.

REFERENCES

1. M. E. WILMS, V. J. GADGIL, J. M. KROUGMAN and B. H. KOLSTER, *Mater. High Temp.* **9**, 3 (1991).
2. G. BERGLAND and P. WIHELMSSON, *Mater. Design* **10**, 1 (1989).
3. R. LOGNEBORG and J. JOHNSON, *Mater. Desigʌ* **10**, 3 (1989).
4. H. SCHLÄPFER and J. WEBER, *Mater. und Technik* **14**, 2 (1986).
5. C. CLARK, P. GENTIL and P. GUHA, *Proc. Int. Conf. Duplex Stainless Steels*, p. 109, The Hague (1986).
6. S. MAKAI, H. OKAMOTO, T. KADO and A. IKEDA, *J. Mater. Energy Sys.* **5**, 1 (1983).
7. A. ASPHAHANI, *Corrosion* **37**, 6 (1981).
8. A. CIGADA, T. PARTORE, P. PEDEFERRI and B. VICENTINI, *Corros. Sci.* **27**, 10 (1987).
9. G. NYSTROM, *Proc. 9th European Cong. Corrosion*, OS-102, Utrecht (1989).
10. Y. MAEHAMA, Y. OHMORI, Y. MARAYAMA, N. TUJINO and T. KUNITAKE, *Metal Sci.* **17**, 11 (1983).
11. S. HERTZMAN, B. LEHTINEN and E. SYMNIOTIS-BARRDAHL, *Proc. Conf. Applications of Stainless Steel '92*, p. 345, Stockholm (1992).
12. J. M. KROUGMAN and F. P. IJSSELING, *Proc. Int. Workshop Electrochemical Corrosion Testing*, p. 135, Ferrara (1985).
13. J. M. KROUGMAN and F. P. IJSSELING, *Proc. 6th Int. Cong. Marine Corrosion and Fouling*, p. 75, Athens (1984).
14. L. SCOPPIO and M. BARTERI, *Proc. Conf. Applications of Stainless Steel '92*, p. 260, Stockholm (1992).